nature materials

REVIEW ARTICLE

PUBLISHED ONLINE: 19 FEBRUARY 2010 | DOI: 10.1038/NMAT2630

Plasmonics for extreme light concentration and manipulation

Jon A. Schuller, Edward S. Barnard, Wenshan Cai, Young Chul Jun, Justin S. White and Mark L. Brongersma*

The unprecedented ability of nanometallic (that is, plasmonic) structures to concentrate light into deep-subwavelength volumes has propelled their use in a vast array of nanophotonics technologies and research endeavours. Plasmonic light concentrators can elegantly interface diffraction-limited dielectric optical components with nanophotonic structures. Passive and active plasmonic devices provide new pathways to generate, guide, modulate and detect light with structures that are similar in size to state-of-the-art electronic devices. With the ability to produce highly confined optical fields, the conventional rules for light–matter interactions need to be re-examined, and researchers are venturing into new regimes of optical physics. In this review we will discuss the basic concepts behind plasmonics-enabled light concentration and manipulation, make an attempt to capture the wide range of activities and excitement in this area, and speculate on possible future directions.

Plasmonics is a flourishing new field of science and technology that exploits the unique optical properties of metallic nanostructures to route and manipulate light at nanometre length scales. Nanometallic objects derive their properties from an ability to support collective electron excitations, known as surface plasmons. At present, plasmonics research enables new fundamental science and device technologies, and we are witnessing a dramatic growth in both the number and scope of plasmonic applications. Plasmonics may soon become a pervasive technology, offering unusual optical capabilities and a tantalizing opportunity to attain unprecedented levels of synergy between optical and electronic functions. Although resistive heating losses in metals can severely limit the performance of devices that depend critically on long-distance propagation of surface plasmon waves (surface plasmon polaritons or SPPs), many useful functionalities have recently been realized despite the presence of loss. The most successful ones tend to use structures for extreme light concentration; plasmonic antennas, lenses and resonators provide excellent examples.

The ability to concentrate light and/or produce high local-field intensities has traditionally been the domain of dielectric lenses and resonators. These objects provide a convenient way to manipulate light and enhance a range of linear and nonlinear phenomena. Owing to the fundamental laws of diffraction, dielectric lenses cannot focus light to spots less than about half a wavelength of light ($\sim\lambda/2$) and dielectric resonators have electromagnetic mode volumes (v_m) limited to $v_m \sim (\lambda/2)^3$, where λ is the wavelength of light inside the dielectric medium. The nature of nanometallic light concentrators and resonators is distinct from their dielectric counterparts, and nanometallic structures do not have these limitations. Plasmonic antennas and lenses can convert optical radiation into intense, engineered, localized field distributions or enable coupling to deep-subwavelength-guided modes. Thus, wherever subwavelength control over light is desired, nanometallic structures are likely to play an important part. By squeezing light into subwavelength volumes, plasmonic structures can efficiently mediate interactions between propagating radiation and nanoscale objects and devices. The first part of this article summarizes the fundamentals behind such plasmonic light concentrators and reviews their use in imaging techniques with improved spatial resolution, ultrafast and compact photodetectors and modulators, higher efficiency solar cells, and techniques for locally controlling catalytic and thermally stimulated processes.

As well as acting as an interface with the nanoscale, plasmonic structures can also change light–matter interactions at a very fundamental level. The possibility to confine light in subwavelength mode-volume cavities has a profound effect on the efficacy of many optical processes that benefit from high-optical-quality factors (Q) and ultrasmall v_m. Despite modest values of Q (typically between 10–100), metallic cavities with sufficiently small mode volumes can often outperform much higher Q dielectric cavities ($Q \sim 10^6$) and benefit from having a more broadband response and easy electrical access. In the second part of this article, we review the use of plasmonic structures to enhance a range of nonlinear processes in ultracompact device geometries, modify the temporal and spatial properties of light emitters, control both near- and far-field thermal radiation pathways, and manipulate light using new optical materials with engineered refractive indices.

In this review, we attempt to describe the very wide range of plasmonic research activities that involve extreme light concentration and manipulation. However, no review of a large field can be exhaustive and we have chosen not to discuss important efforts on plasmon-based sensors, which constitute a large body of research for which excellent recent reviews already exist[1].

Fundamentals of plasmonic light concentrators

Researchers are investigating the optical properties of an increasing variety of metallic nanostructures with the hope of effectively concentrating light into nanoscale volumes. The structures come in two distinct varieties: resonant and non-resonant. In resonant structures, time-varying electric fields associated with light waves exert a force on the gas of negatively charged electrons inside a metal and drive them into a collective oscillation, known as a surface plasmon. At specific optical frequencies this oscillation is resonantly driven to produce a very strong charge displacement and associated (light) field concentration. We will first discuss such resonant behaviour in quasistatic and retardation-based structures, before continuing with non-resonant objects.

The quasistatic approximation for electromagnetics is valid when the size of a nanostructure is significantly smaller than the

Geballe Laboratory for Advanced Materials, Stanford, California 94305, USA. *e-mail: brongersma@stanford.edu

free-space wavelength of the incident light, such that the entire structure experiences a uniform electric field at any instant of time. In this regime, resonance effects can be determined by solving for the electrostatic potential for a structure of given geometry and dielectric constant embedded within a uniform electric field. Spherical nanoparticles, for instance, exhibit a dipolar plasmonic resonance at wavelengths where $\varepsilon_m = -2\varepsilon_d$, where ε_m and ε_d are the permittivities of the metal and dielectric, respectively. Although quasistatic resonance frequencies are independent of particle size, metallic nanoparticles can be made resonant over a wide range of frequencies by changing the type of metal, particle shape or dielectric environment (Fig. 1a,b). A number of very general, geometry independent results can be derived for these resonators. For instance, plasmon resonance occurs at a frequency where the energy

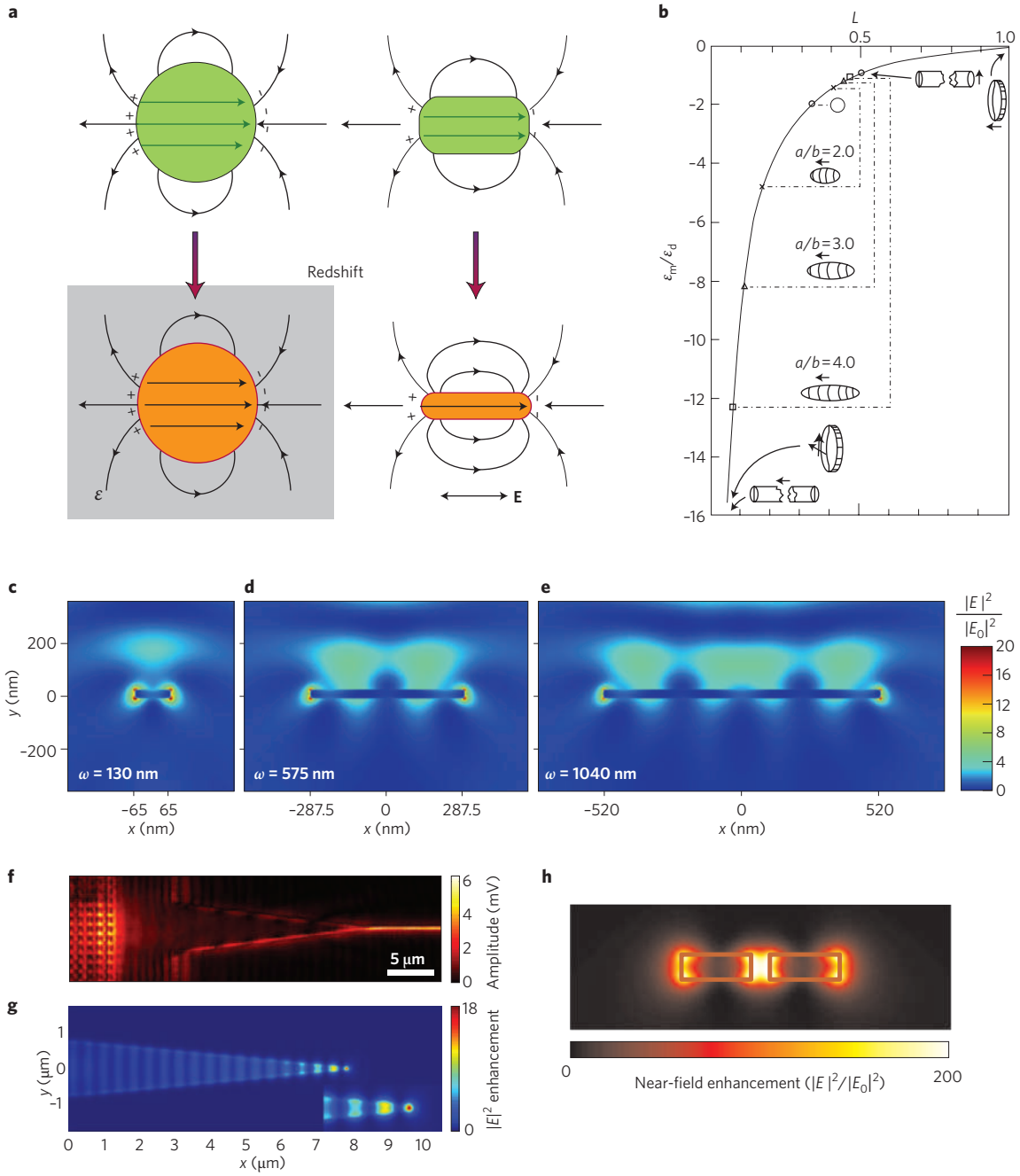

Figure 1 | Fundamentals of plasmonic-light concentrators and resonators. a, Effects of geometry and materials on electrostatic resonances of deep-subwavelength metal nanostructures. As the surrounding dielectric constant is increased the resonance for a spherical nanoparticle (shown on the left) redshifts. As the aspect ratio for a nanorod is increased the longitudinal resonance is redshifted (shown on the right)[2]. Minus (plus) signs indicate regions of high (low) electron density. **b**, Resonant condition ($\varepsilon_m/\varepsilon_d$) as a function of aspect-ratio parameter L for quasistatic spheroidal particles, which are shown as inset[116]. The major and minor axes of the spheroid are represented by a and b, respectively. **c**–**e**, Retardation-based strip resonators. Normalized field-intensity distributions normalized to incident intensity for the lowest odd-order resonances of 30-nm-thick silver strips that are top-illuminated with light at wavelength of $\lambda_0 = 550$ nm. E_0 denotes the incident electric-field strength. Three different resonant antennas are shown that approximately measure one (**c**), three (**d**) and five (**e**) times $\lambda_{SPP}/2$ (ref. 10). **f**,**g**, NSOM measurements (**f**) and finite difference time domain simulations (**g**) illustrating SPP focusing using a tapered metal strip waveguide[117]. **h**, Large near-field enhancement in the feed-gap of a gold optical antenna[118]. Figures reproduced with permission: **a**, © 2006 APS; **b**, © 1998 Wiley; © **c**–**g**, 2008 OSA; **h**, © 2005 AAAS.

inside the metal and surrounding dielectric is equal[2]. Furthermore, their Q value is solely determined by the metal losses at the resonant frequency and cannot be altered by modifying geometry[2]. Whereas single subwavelength particles can provide field enhancements of 10–100, placement of subwavelength particles in fractal aggregates[3] or self-similar chains[4] can provide field enhancements at least one order of magnitude larger.

When nanostructures have one or more dimensions approaching the excitation wavelength, the optical phase can vary across the structure and it is necessary to consider retardation effects. The concepts behind many retardation-based plasmonic light concentrators are based on scaled radiofrequency antenna designs, such as the half-wavelength dipole antenna. Such scaling is non-trivial as metals show finite conductivity and support SPPs at optical frequencies. Wavelength-scale nanometallic structures, such as metal nanowires[5–7] or strips[8,9] can be considered as truncated SPP waveguides. Surface plasmon polaritons propagate back and forth between the metal terminations, creating a Fabry–Perot resonator for SPPs. To first order, the resonant length of such structures is therefore equal to $n\lambda_{SPP}/2$, where n is an integer and λ_{SPP} is the wavelength of the supported SPP mode (Fig. 1c–e). In practice, the phase pick-up on reflection from the metal termination is non-negligible and can give rise to substantial changes in the resonant length[9,10]. These concepts can easily be extended to plasmonic waveguides consisting of two parallel-running metal structures to realize metal–dielectric–metal (MDM) cavities. As the MDM modes are not cut off when the metal-to-metal spacing is reduced, fields can be concentrated effectively in truly nanoscale volumes[11].

Owing to the small size of the resonators described above, dielectric lenses are typically required to efficiently couple free-space light to the structure of interest. However, plasmonic structures can also concentrate light from areas that are substantially larger than the wavelength of light. In a plasmonic lens, an engineered grating first couples free-space photons to SPPs that then funnel energy towards a central focus. If light hits a grating with a grating constant G, it can gain a momentum in multiples of $2\pi/G$ in the direction of the periodicity and allow the coupling to higher momentum SPPs[12,13].

Non-resonant effects can also be used to further enhance light concentration. For instance, strong subwavelength light localization in retardation-based resonators can be achieved by introducing a small gap in the metal structure, known as a feed-gap (Fig. 1h)[14]. Here, one takes advantage of the fact that SPPs have an appreciable longitudinal electric-field component (normal to the gap) that jumps inside the gap by the ratio $\varepsilon_m/\varepsilon_d$ (owing to the electromagnetic boundary condition that requires the normal component of $\varepsilon\mathbf{E}$, where $\mathbf{E}$ is the electric-field vector, to be continuous across the metal/dielectric interface)[9]. A more physical interpretation attributes the high local fields to the build-up of charges of opposite sign across the gap. Similar broadband dielectric contrast-based enhancements of local-field intensities can be achieved through 'lightning rod' effects. The lightning-rod effect occurs at a sharp metal termination, where field-continuity conditions force surface charges into a small area. The effect can be described with electrostatics[15], but can also be used in unison with other field-enhancement strategies in larger retardation-based structures. Finally, we note that plasmonic tapers, such as metal cones or wedges, can also provide broadband, non-resonant enhancements. Such structures support SPP waves that show an increase in wavevector and a decrease in group velocity as they propagate towards their apex[16,17]. As a result, an SPP launched near the base of a structure experiences considerable field concentration as it propagates towards the tip (Fig. 1f,g).

Near-field scanning optical microscopy

Subwavelength optical imaging has been among the first practical applications of plasmonics and its positive impact on the development of the field has been tremendous. Early demonstrations of near-field scanning optical microscopy (NSOM) used subwavelength apertures in metal-coated optical probes. Unlike conventional microscopy, these aperture-based systems show a spatial resolution determined by the aperture size rather than the wavelength of light. Unfortunately, minimum aperture dimensions are limited by optical throughput; the power transmitted through a subwavelength aperture scales inversely with the square of the aperture area[18]. New aperture designs such as C-shapes[19] can drastically increase the transmitted power for a given near-field spot size, a result that has proven important for various scanning near-field technologies. The ability to create highly localized fields may also have broad implications for optical trapping[20], the next generation of data storage[21] and photolithography[22] (Fig. 2a). For these applications, the integration of plasmonic structures with scanning components enables precise control over intense nanoscale optical fields while minimizing the presence of unwanted diffraction-limited background light.

The limitations set forth by aperture throughput can be circumvented with apertureless techniques. In apertureless NSOM (aNSOM), for instance, a sharp metal tip is illuminated by a light source polarized along the tip's long axis. The lightning-rod effect generates an intense near-field spot localized at the tip's apex, which is superimposed on a broad diffraction-limited spot. Effects owing to the non-localized background can be suppressed using nonlinear optical effects or distance-dependent demodulation techniques. The resolution of aNSOM is in large part determined by tip radius, and deep-subwavelength (λ/3,000) spatial resolution[23] imaging is feasible especially at infrared and terahertz frequencies (Fig. 2c). This concept has recently enabled high-resolution imaging and spectroscopy on structures as small as carbon nanotubes[24] (Fig. 2b) and DNA[25]. The aNSOM technique is not limited to sharp metal tips and

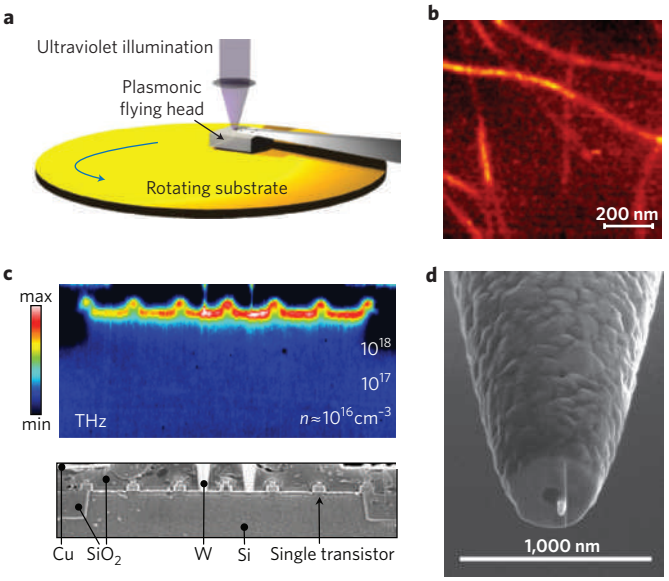

Figure 2 | Plasmon-based subwavelength imaging and photolithography. **a**, Schematic of a plasmonic nanolithography system. An array of plasmonic bull's-eye aperture lenses are located at the end of a write-head and focus ultraviolet light to spots of roughly 100 nm. The head is kept within a distance of 30 nm from the rotating substrate using an air bearing[22]. **b**, A near-field Raman image taken from several carbon nanotubes by detecting the intensity of the 'G' band on laser excitation at 633 nm. **c**, An aNSOM image of a multiple transistor structure cross-section. The terahertz illumination (λ = 118 nm) can distinguish between regions of differing dopant density (n) and can resolve the structure of individual transistors with a resolution of roughly 40 nm. **d**, An SEM image of a TOA probe[28]. Figures reproduced with permission: **a**, © 2008 NPG; **b**, © 2003 APS; **c**, © 2008 ACS; **d**, © 2007 ACS.

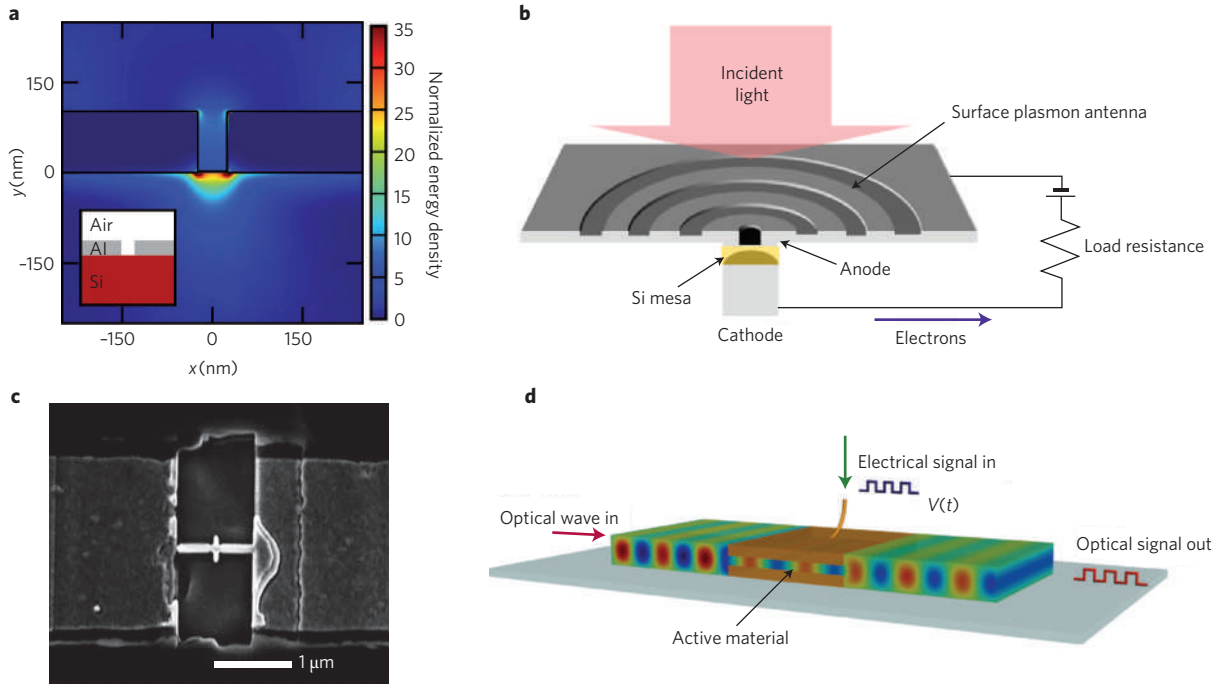

Figure 3 | Plasmon-based detectors and modulators. a, Normalized field-energy density for a single isolated slit of 50 nm width in a 100-nm-thick aluminium film on a silicon substrate (shown as inset), top-illuminated by a plane wave (λ = 633 nm) polarized in the *x* direction[30]. **b**, Concentric grating coupler used to funnel SPPs towards a central Si photodetector[31]. **c**, Plasmon-enhanced Ge photodetector using a sleeve-dipole antenna to concentrate a near-infrared signal beam at 1310 nm (ref. 32). **d**, Schematic of a plasmonic modulator capable of encoding electrical signals into an optical data stream by applying a signal voltage $V(t)$ across a nonlinear medium sandwiched between two metallic plates (which are shown in orange). Figures reproduced with permission: **a**, © 2009 OSA; **b**, © 2005 JSAP; **c**, © 2008 NPG.

alternative configurations have used different light-concentrating structures including metal nanoparticles[26] and bowtie antennas[27].

The tip-on-aperture (TOA) approach is a particularly interesting probe geometry that has emerged recently. Here, a metal protrusion is deposited adjacent to an NSOM aperture, further localizing the aperture fields. Tip-on-aperture combines the background suppression of conventional apertures with the enhanced fields and tip-limited resolution of apertureless techniques. Initial TOA techniques achieved field enhancements owing to tip sharpness only[25]. Later, researchers optimized tip length to fully take advantage of retardation effects[28] (Fig. 2d). Although primarily used in near-field microscopy, the TOA method could prove useful for a diversity of technologies that require light to be delivered to extremely small volumes.

Photodetectors

The ability of plasmonic structures to manipulate light well below the classical diffraction limit is giving rise to a myriad of new chip-scale photonic components. The integration of plasmonic structures with existing electronic and dielectric devices can be realized by an increasing number of nanofabrication techniques, including mature silicon-integrated-circuit technology. Of the many emerging applications, plasmon-enhanced photodetectors are particularly promising.

At present, our ability to shrink conventional photodetectors is constrained in the lateral dimensions by the diffraction limit and in the vertical dimension by the finite absorption depth of semiconductors. These size limitations significantly affect detector performance. Reducing detector size below these limits would result in increased speed, decreased noise and reduced power consumption. The speed of a detector is generally limited either by its carrier-transit time (the time it takes photogenerated carriers to transit the detector's intrinsic region), or resistor–capacitor (RC) time constant (the time required to charge the device's effective capacitance, C). Whereas the carrier-transit time scales with the length of the device, the RC time constant and power consumption are all proportional to device capacitance and thus scale roughly with device area. To achieve projected integrated-circuit operating speeds of 40 GHz, a 50 Ω RC-limited device requires a capacitance less than ~0.1 pF. An even lower limit on device capacitance of about 10 fF arises from constraints on power consumption[29], which scales with operation frequency f as ~ $0.5\,fCV^2$, where V is the voltage. The requirements on high-speed and low-power necessitate ever-shrinking device dimensions. As plasmonic structures can concentrate light both laterally and in the depth of a semiconductor material (Fig. 3a), they are ideally suited to this task[30].

The ability of resonant plasmonic structures to efficiently concentrate light into a deep-subwavelength-detector region was demonstrated[31] in pioneering work that used a 10 μm diameter concentric grating coupler (see Box 1) to funnel SPPs towards a central silicon photodetector (Fig. 3b). The coupler improved the detector's photoresponse by more than a factor of 20 and its miniscule size resulted in a very fast response time (20 ps, full-width at half-maximum) and a low capacitance (< 15 fF).

An alternative plasmon-enhanced detector[32] with an even smaller physical extent is shown in Fig. 3c; the device consists of a deep-subwavelength volume of germanium embedded in the arms of a sleeve-dipole antenna designed to be resonant in the near infrared (1310 nm). Resonant antenna effects were observed by measuring the photoresponse for light polarized parallel and perpendicular to the dipole antenna, with an observed polarization contrast ratio up to 20. The small total footprint of this device and its record-low active semiconductor volume of $10^{-4}\,\lambda^3$ naturally lend themselves to dense integration. Plasmonic waveguide-based detectors have also recently been demonstrated and offer valuable integration advantages[33–35].

By using metallic nanostructures as a bridge between dielectric microphotonics and nanoscale electronics, one plays to the strengths of both the metallic nanostructures (concentrating fields and sub-wavelength guiding) and semiconductor electronic components

(high-speed and high-performance information processing). Plasmonics also offers the possibility of introducing new functionality, including polarization, angle or wavelength selectivity[36].

Modulators

As well as photodetectors, the realization of a complete chip-scale optical link will require high-speed and power-efficient optical

Box 1 | A macroscopic light concentrator based on transformation optics

To create a light concentrator, we need to squeeze the optical space in a given region and therefore enhance the electromagnetic energy density within that area. For example, when a two-dimensional cylindrical system is considered, one needs an appropriate transformation function that compresses a cylindrical region of $r < b$ (where r is the original coordination system, and b (as well as a and c) is a geometrical parameter) into a smaller cylinder of $r < a$. In this case the incident plane wave will be concentrated to the inner cylinder, and the energy density there will be increased by a factor of $(b/a)^2$. A larger cylinder of $r < c$ is necessary to complete the coordinate change (panel **a**).

Next, a spatial transformation is required that takes us from r to the redesigned system (r'). Although there are countless possibilities, a linear function as shown in panel **b** is considered here. After settling on the desired transformation function, the ε and μ tensors can be determined using standard techniques in transformation optics[119]. The calculated anisotropic material properties for the proposed light concentrator are plotted in panel **c**. The two material tensors are identical, a feature common to any ideal transformation-based devices.

To illustrate the device performance, we plot a full-wave simulation (panel **d**) for a light concentrator working at $\lambda = 1.5$ μm with geometrical parameters of $a = 1$ μm, $b = 5$ μm and $c = 8$ μm (grey steamlines represent the time-averaged power flow). A transverse magnetic incident wave with its magnetic field polarized along the cylindrical axis is assumed in the simulation. Although the magnetic-field magnitude remains uniform throughout the whole space, the field density is enhanced substantially in the region of $r < a$. The time-averaged normalized energy density (panel **e**) within the inner cylinder region increases by a factor of $(b/a)^2 = 25$ at the expense of a reduced energy density in the annular region of $b < r < c$.

The practical application of such a device does not require all optical parameters to follow the predescribed dependencies shown in panel **c**. For example, under the transverse magnetic illumination described above, only μ_z, ε_θ and ε_r are necessary, whereas the other three are irrelevant. Moreover, tricks using advanced transformations and normalization techniques[120] can further simplify the design with only a slight decrease in performance.

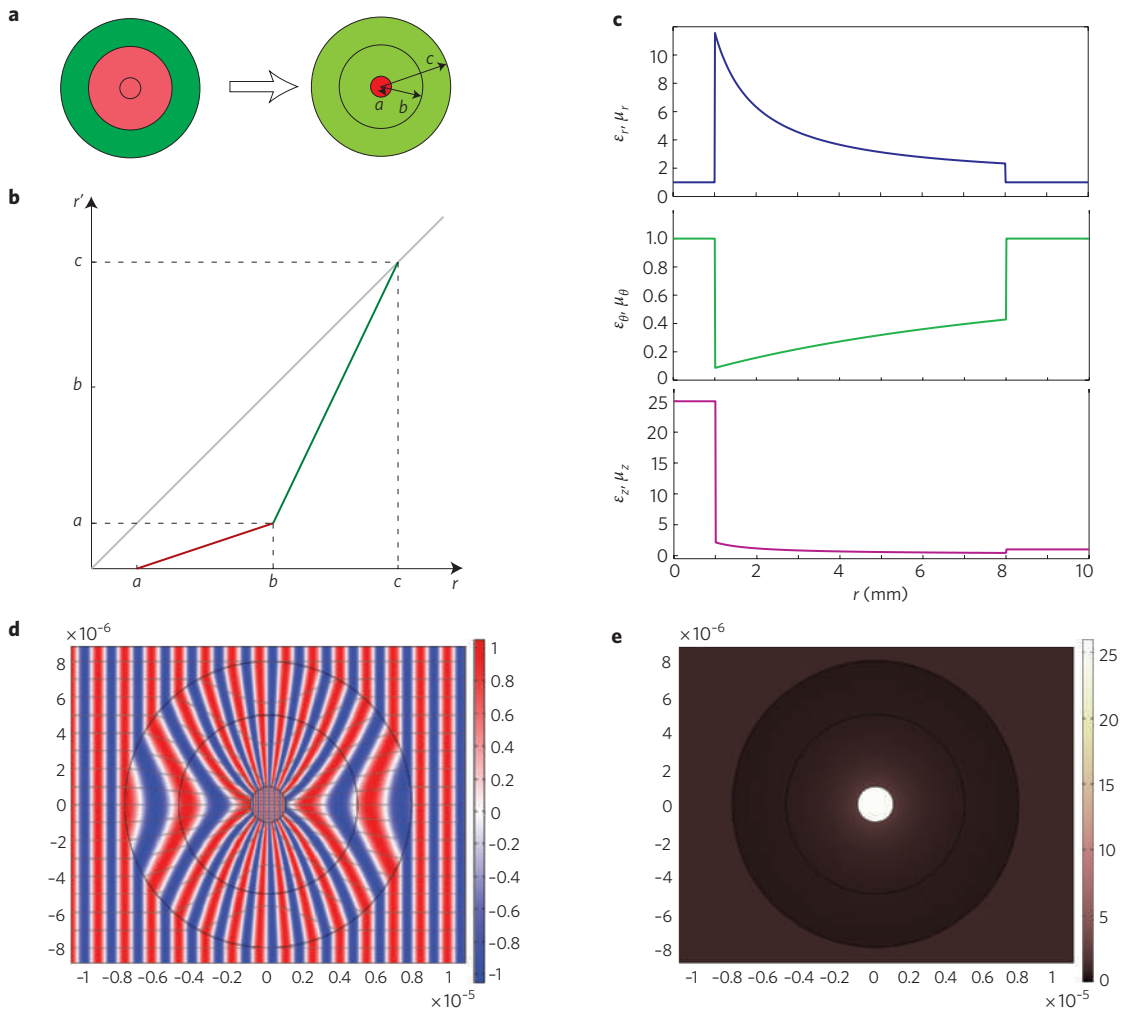

modulators. The scaling of present complementary metal oxide semiconductor modulator designs to micrometre-scale dimensions is hampered by weak nonlinear optical effects in Si-compatible materials. Plasmonics could allow radically new modulator designs that are substantially more compact and thus power efficient. Pioneering studies of long-range-SPP mode modulators, which act on the coupled-interface SPP mode supported by thin metal stripes, have demonstrated two key advantages conferred by plasmonics. First, plasmonic modulators can use the same metal circuitry to perform simultaneous electrical and optical functions; the metal stripes can guide an SPP signal and transmit electrical control pulses to switch the SPP signal[37]. Second, the high field confinement of SPPs near the metal can be used to attain excellent mode overlap with the surrounding active media, inducing a boost in the nonlinear response. For example, plasmonic thermo-optic modulators can show higher extinction ratios (> 30 dB) and lower driving powers (~10 mW) than dielectric-waveguide-based counterparts[37]. Despite these advantages, the application potential of long-range-SPP-based modulators is severely limited by their large sizes, which gives rise to issues with dense integration and power consumption (scales with capacitance and thus area).

By moving to an MDM waveguide geometry, however, the advantages conferred by plasmonics can be achieved within a nanoscale device. A conceptual schematic of a model nanoscale plasmonic modulator is shown in Fig. 3d. Such a device is capable of encoding electrical signals into an optical data stream by dramatically changing the optical properties of a nonlinear optical medium sandwiched between the metal plates of a MDM plasmonic waveguide. As MDM waveguides do not exhibit cut-off, the metal-to-metal spacing can be very small (a few tens of nanometres) and low voltage swings can produce large swings in the electric fields and thus strong nonlinear effects. The excellent overlap of the MDM modes with the active medium further aids in realizing efficient, low-power switching. Whereas high-confinement plasmonic waveguide structures are severely limited by the rapid attenuation of the SPP waves, there may well be a range of viable applications for modulators and other active plasmonic components. As long as the nonlinearities are strong enough, these devices can be small compared with characteristic decay lengths of SPPs such that their performance is only weakly affected by unavoidable resistive losses in the metals. For modulators, optically induced absorption-depth swings exceeding several 1000 cm^{-1} will be required to enable manageable modulation amplitudes (~3 dB) and device transmission losses (~3 dB) for chip-scale applications[38]. Such materials are at present tested in all optical switching configurations[39–42] and in electrically controlled devices[43]. In parallel with these advances, significant progress has also been made in accelerating modulators to enable terahertz modulation bandwidths[44] and in using optical bistability for potential optical logic applications[45].

Photovoltaics

Photovoltaic cells can provide virtually unlimited amounts of energy by effectively converting sunlight into clean electrical power. Large-scale implementation of photovoltaic technology hinges on our ability to produce high-efficiency modules in an inexpensive and environmentally friendly fashion. Thin-film solar cells may provide a viable pathway towards this goal by offering low materials and processing costs[46]. The energy conversion efficiencies of such cells are still fairly low owing to the large mismatch between electronic and photonic length scales in these devices; for photon energies close to the bandgap, the absorption depth of light in semiconductors is significantly longer than the electronic (minority carrier or exciton) diffusion length in most deposited thin-film materials. As a result, thin cells that offer efficient charge extraction fail to efficiently capture the sunlight that falls on them.

Plasmonic nanostructures may provide a materials-agnostic strategy to solve the issue above by dramatically improving light absorption in a wide range of thin-film photovoltaic cells; the relevant concepts are discussed in a review of this topic in this issue of *Nature Materials*[47]. Many advances have been made since researchers first proposed the use of plasmonics to boost photovoltaic cell efficiencies more than a decade ago[48,49]. Present research is focused on taking advantage of (1) the high near-fields surrounding metallic nanostructures close to their surface plasmon resonance frequency and (2) effective light trapping in the active semiconductor layer to boost light absorption[50]. This requires a detailed optimization of the nanostructure size, shape and spacing that is unique to each specific cell type[51].

Catalysis and thermal management

Metallic nanostructures have an equally vital role in the chemical industry as they do in the field of plasmonics. There, they serve as catalysts that allow a wide variety of chemical reactions that are invaluable to modern-day life. A merging of the fields of plasmonics and catalysis thus seems natural and extremely beneficial. In 1981, Nitzan and Brus argued that the electromagnetic-field concentration afforded by surface plasmons should enhance the rate of photochemical reactions[52]. Soon thereafter, this was demonstrated for the photodissociation of dimethyl cadmium[53]. In the future, plasmon-enhanced light concentration can provide improved light management for a wide range of photocatalytic reactions (for example, water splitting for hydrogen production) and allow more effective photocarrier generation near reactive surfaces. *In situ* surface plasmon spectroscopy techniques have also enabled new ways to study reactions in small volumes, such as molecular junctions[54]. Recent progress in this area has even enabled quantification of reaction rates and atomic deposition processes down to the level of individual metal nanoparticles[55]. These studies have provided new insights into the impact of the catalyst structure on the catalytic process and offer new approaches to explain complex dynamic behaviour on the surface of nanostructured catalysts.

Light-induced heat generation in metals can also be used to control chemical reactions and thermally activated physical processes (that are potentially far out of equilibrium). Whereas in many plasmonics applications the generation of heat is undesirable, the ability to rapidly raise and lower the temperature in nanoscale volumes of material can be used to control chemical reactions with unprecedented spatial and temporal control. Metallic nanostructures are effective, light-driven sources of heat owing to their large optical absorption cross-section. By engineering the size, shape and dielectric environment of metallic particles one can control their ability to absorb and scatter light[56]. New methods to accurately measure the local temperature near hot metallic nanostructures are being developed and keep increasing in accuracy[57]. This effective heating has resulted in many plasmonics applications, including selective identification and killing of cancer cells[58]; modification of polymer surfaces[59]; local control over phase transitions[60,61]; growth of individual semiconductor nanowires and carbon nanotubes[62]; nanofluidics and chemical separation[63]; drug delivery[64]; and induced reversible photothermal melting of DNA[65,66]. In many of these applications the need to heat only locally rather than globally has resulted in significant increases in control, speed and energy efficiency with an accompanying reduction in cost.

Nonlinear optics

As light concentrators can substantially boost the field intensity within a prescribed region, it is therefore natural to consider their involvement in nonlinear optics. Plasmonic antennas have indeed been used to enhance the efficiency of various nonlinear optical processes; second-harmonic generation (SHG) in patterned metal films has been studied in the most detail. Although noble metals are centrosymmetric media lacking a bulk SHG capability, the broken

symmetry at metallic surfaces allows for SHG processes. Because the nonlinear cross-section scales with the square of the optical intensity, SHG at metal interfaces can be increased by more than an order of magnitude through coupling to SPPs[67]. Patterned metal films, such as periodic arrays of subwavelength apertures, can further increase the electromagnetic intensity and SHG. The first experimental demonstration of such effects was carried out using a silver bull's-eye collector, where a ~10^4 increase in the frequency doubling efficiency was achieved owing to the enhanced and localized transmittance[68]. Similar enhancement of SHG efficiency in metal films has been observed in other light-concentrating geometries, including overlapping double holes[69], periodic rectangular holes[70], and disordered aperture arrays[71]. The scanning electron micrograph (SEM) images of several structures for frequency doubling enhancement are shown in Fig. 4a-d.

Plasmonic structures can also enhance nonlinear effects by concentrating light into nonlinear media placed directly within a field-enhancement region. It has been reported that the SHG efficiency from nanopatterned GaAs located in gap of a subwavelength coaxial structure (Fig. 4e) can be two orders of magnitude larger than that from conventional bulk nonlinear materials such as $LiNbO_3$ (ref. 72). Similar results were obtained with GaAs inside metallic hole arrays[73]. Recently, using modest pump intensities of 10^{11} W cm^{-2}, up to seventeenth-order harmonics (corresponding to an extreme ultraviolet wavelength of 47 nm) were produced in argon gas within the feed-gap of gold bowtie nanoantennas[74]. The schematic for the light–argon interaction and the SEM image of the bowtie antennas for extreme-ultraviolet generation are presented in Fig. 4f,g. Regardless of the exact structures used, it is clear that engineered plasmonic light concentrators have the potential to drastically enhance a wide variety of nonlinear optical interactions, although the maximum attainable enhancements are as of yet unclear.

Engineering radiative decay

The strongly confined fields near metallic nanostructures can profoundly alter the light-emission properties of nearby optical emitters[75,76] by: (1) increasing optical excitation rates; (2) modifying radiative and non-radiative decay rates; and (3) altering emission directionality. For optical pumping below saturation, the fluorescence rate γ_{em} can be expressed as $\gamma_{em} = \gamma_{exc}[\gamma_{rad}/(\gamma_{rad} + \gamma_{non\text{-}rad})]$, where γ_{exc} is the excitation rate and γ_{rad} and $\gamma_{non\text{-}rad}$ are the radiative and non-radiative decay rates, respectively. Assuming an emitter's internal quantum structure remains unchanged, light-concentrating structures can increase the optical absorption rate ($\gamma_{exc} \propto |\mathbf{p} \cdot \mathbf{E}|^2$), where $\mathbf{p}$ is the dipole moment and $\mathbf{E}$ is the optical electric-field vector, owing to enhanced excitation fields at the emitter position, and thus increase photoluminescence intensity. These structures can also affect the relaxation of excited emitters back to their ground state by introducing new electromagnetic decay pathways; according to the Purcell effect, spontaneous emission is not an intrinsic property of an emitter and can be affected by the surrounding electromagnetic environment. In terms of typical cavity quantum electrodynamics, plasmonic nanostructures exhibit only moderate values of Q (~10–100). However, the mode volumes v_m can be much smaller than a typical dielectric cavity, $v_m \sim (\lambda/2)^3$, and the resulting Purcell factor ($F_p \propto Q/v_m$) can be large enough to observe significant lifetime reductions.

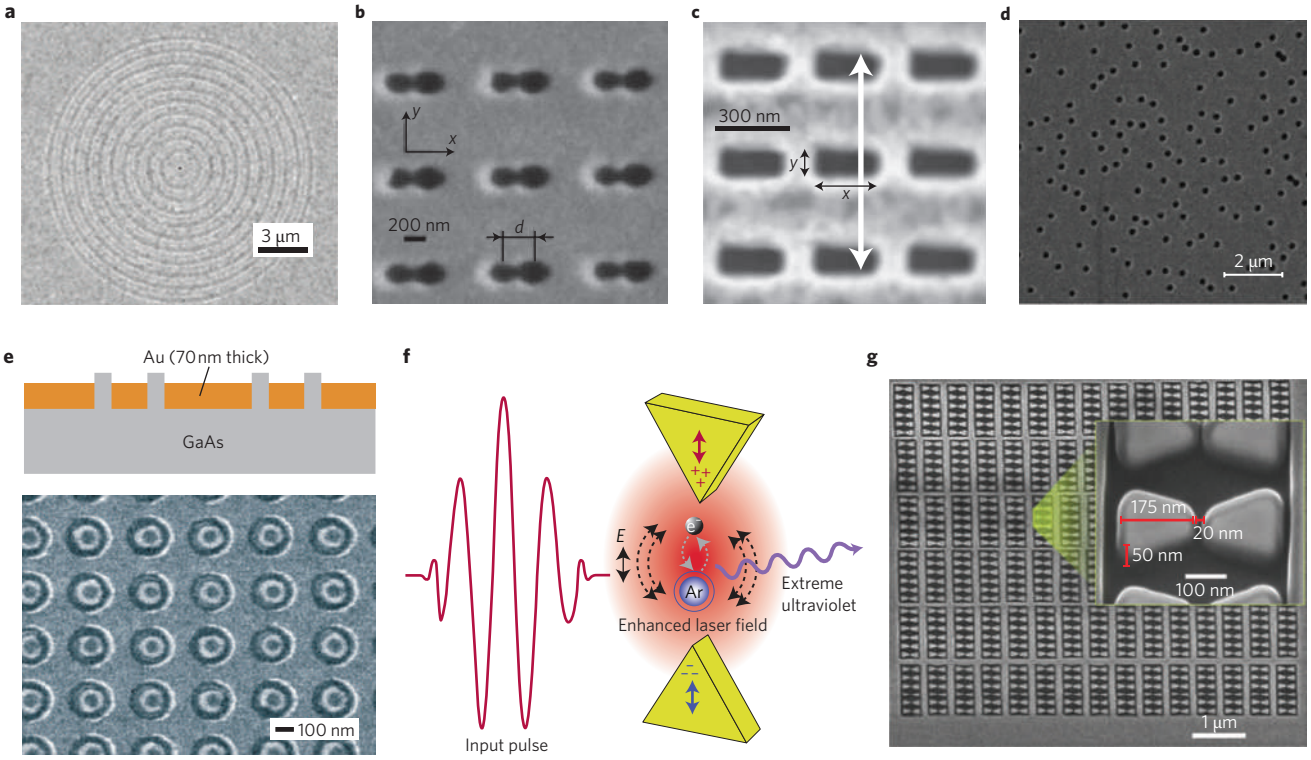

Figure 4 | Light-concentration structures for strengthening nonlinear optical interactions. a–d, Patterned metal films with enhanced SHG in metallic structures for fundamental wavelength of about 800 nm, including the bull's eye[67] (**a**); overlapping double holes[68] (**b**); periodic rectangular holes[69] (**c**) (the white arrow corresponds to the polarization of incident light); and disordered aperture arrays[70] (**d**). **e–g**, Enhanced frequency conversion in nonlinear media located within the field-enhanced region, including enhanced SHG from GaAs in a nanocoaxial structure[71] for a fundamental wavelength of ~3 μm (**e**); schematic (**f**) and SEM image (**g**) of nano-bowtie antennas for extreme-ultraviolet generation[73] using a standard Ti:sapphire laser. The enhanced laser fields accelerate electrons (e^-) around an argon (Ar) atom, generating extreme-ultraviolet radiation. Figures reproduced with permission: **a**, © 2003 OSA; **b**, © 2006 AIP; **c**, © 2006 APS; **d**, © 2007 OSA; **e**, © 2006 ACS; **f**,**g**, © 2008 NPG.

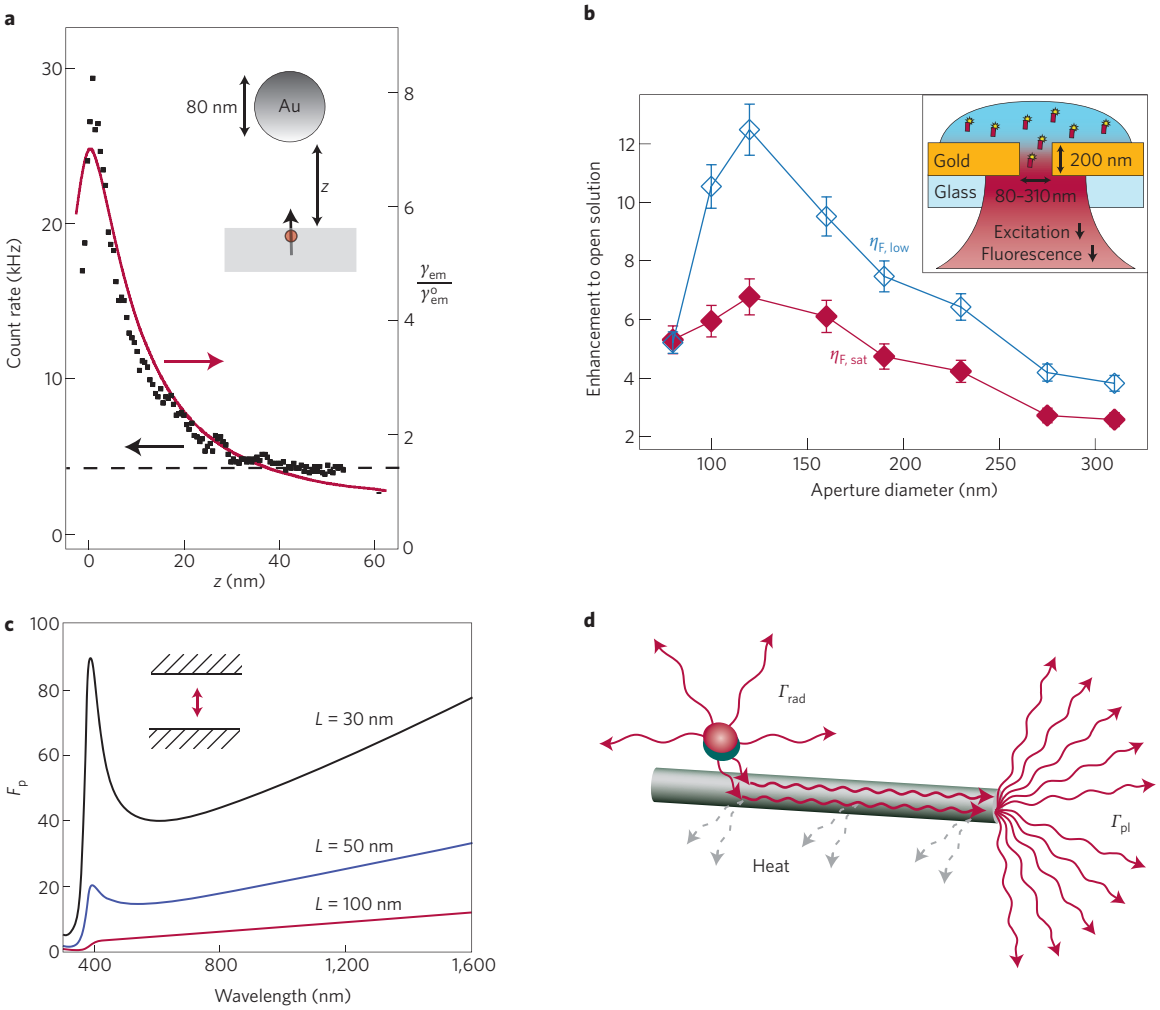

Figure 5 | Radiative-decay engineering and quantum plasmonics. a, Fluorescence rate (γ_{em}) of a vertically oriented molecule near a metal nanoparticle as a function of particle–surface distance (z) normalized by the rate in the absence of the nanoparticle (γ^0_{em}). The fluorescence enhancement reaches a maximum at a distance of $z \approx 5$ nm. For shorter distances, fluorescence is quenched (red curve: theory; black dots: experiment)[74]. **b**, Fluorescence enhancement of a single molecule in a metal nanohole as a function of hole diameter (red curve: at fluorescence saturation ($\eta_{F,sat}$); blue curve: below saturation ($\eta_{F,low}$)). Error bars indicate the standard deviation of measurements and numerical fitting. The enhancement difference between the red and blue curves results from the respective influence of the excitation intensity enhancement and lifetime reduction[79]. **c**, Spontaneous emission enhancement of a dipole source in an MDM slab as a function of emission wavelength. The dipole source is in the centre of the gap and oscillates normal to the interfaces. As the gap size L (shown as inset) decreases, the enhancement factor (F_P) increases rapidly[83]. **d**, Generation of guided single plasmons (shown in red) along a silver nanowire[86]. Γ_{rad} and Γ_{pl} refer to the spontaneous emission rate of a coupled quantum dot into free space or guided surface plasmons, respectively. Figures reproduced with permission: **a**, © 2006 APS; **b**, © 2008 OSA; **c**, © 2008 APS; **d**, © 2007 NPG.

When located near metal nanoparticles, excited molecules relax rapidly by exciting localized surface plasmons by means of near-field coupling. The total decay rate ($\gamma_{rad} + \gamma_{non\text{-}rad}$) can increase by a considerable degree owing to the large local density of optical states (LDOS) near the metal surface. Particularly large enhancements are obtained when the molecular emission frequency matches the surface plasmon resonance frequency of the nanoparticle or if fields are squeezed into a smaller volume by coupling to a second nanoparticle[77]. Once excited, localized surface plasmons can either decay non-radiatively because of internal damping, or re-radiate into free space. Depending on a variety of parameters, coupled molecule–nanoparticle systems can exhibit either increased or decreased (quenching) luminescence[75,76,78], as shown in Fig. 5a. For most applications it is desirable that metal nanoparticles behave in a similar way to optical antennas — increasing luminescence yields by obtaining energy from nearby emitters and redistributing it to the far-field. Recently, it was also demonstrated that the angular emission of a single molecule near a metal nanoparticle (that is, optical antenna) follows the antenna mode, regardless of the molecular orientation[79]. Thus, properly designed metal nanoparticles can both increase light output and redirect light emission into preferred directions, resulting in a superior class of light emitter.

Subwavelength metal holes can also enhance excitation and decay rates of embedded emitters by means of coupling to guided SPP modes. Depending on the hole diameter, these two effects may have varying contribution to the total fluorescence enhancement[80] (Fig. 5b). The observed enhancement is largest around the cutoff of the fundamental guided mode of the excitation field, where the group velocity is minimized and the LDOS is maximized. By using nanoholes to restrict excitation and collection to a nanoscale volume, researchers can now perform fluorescence-based single-molecule detection at high, micromolar concentrations[81].

Localized surface plasmons in metal nanoparticles and holes couple to only a small number of nearby emitters and are useful for single-molecule spectroscopy. Propagating SPPs on metal films, on the other hand, can affect light emission over large

areas and are more suitable for solid-state lighting. Spontaneous emission enhancements of quantum well semiconductor emitters in the vicinity of metal films were studied experimentally[82] and plasmon-enhanced light-emitting diodes were demonstrated[83]. When the plasmon resonance frequency ($\varepsilon_m \rightarrow -\varepsilon_d$) of a metal film matches the quantum well emission frequency, there is a large enhancement in photoluminescence intensity that could permit more efficient solid-state lighting. However, resonant enhancement effects require spectral tuning owing to their limited bandwidth. The large metal losses around the surface plasmon resonance frequency also impose limitations on practical applications. Recently, it was shown that emitters in MDM structures can exhibit large spontaneous emission enhancements even at non-resonant (that is, broadband) conditions, owing to the tight confinement of modes between two metallic films[84] (Fig. 5c). These large enhancements cause emission to be preferentially directed into plasmonic waveguide modes, which can then be out-coupled into free-space or dielectric waveguides. Thus, MDM structures may be useful for building efficient on-chip light sources for integrated optics.

In plasmonic structures with sufficiently small mode volumes, it may ultimately become possible to reach a regime where coherent interactions between an SPP mode and atomic system can be used for quantum optics applications[85]. Recent proposals suggest that a metal nanowire coupled to a three-level emitter could act as a single-photon transistor. In such a device, an optical signal consisting of a stream of single SPPs is controlled through a low-intensity optical gate[86]. Recent experiments have demonstrated significant progress towards this goal. By coupling CdSe quantum dots to a silver nanowire, researchers have demonstrated the ability to generate single SPPs with an estimated efficiency greater than 50% (see Fig. 5d)[87]. The use of small-mode-volume light concentrators for quantum optics applications represents an exciting frontier in the field of plasmonics.

Based on the many successes in coupling between emitters and metallic nanostructures, it is no surprise that scientists are now investigating the use of metallic structures to realize nanoscale lasers. Nanocavity lasers based on electrically pumped metal-coated cavities[88], MDM waveguides[89], or optically pumped hybrid plasmon–semiconductor–nanowire modes[90] have been demonstrated. Although the laser emission in those devices was coupled to far-field radiation, we may soon see implementations of near-field lasers. In the proposed surface plasmon amplification by stimulated emission of radiation (spaser), light is coherently emitted into a localized surface plasmon mode[91,92]. In a spaser, the lasing mode may even be a non-radiating dark state, generating a coherent, background-free nanoscale light source. Recent work discusses the experimental implementation of such an intriguing device[93]. Successful implementations of spasers may lead to new applications in nanoscale sensing and lithography.

Thermal emitters

Extension of radiative-decay engineering concepts (Purcell enhancements) to longer wavelengths (mid-infrared) is hampered by a lack of suitable light-emitting materials. Luckily, plasmonic structures can themselves be made to emit light in a carefully engineered fashion. The thermal radiation from a heated structure obeys Kirchhoff's law of thermal radiation: the object's emissivity (e) is equal to its absorptivity (A) at all frequencies (ω) and angles (θ), that is $e(\theta,\omega) = A(\theta,\omega)$. Whereas metals are typically weak emitters (absorbers) at infrared frequencies, they can be engineered to serve as narrow-band, size-tunable emitters when structured into arrays of microstrip patch antennas[94] (Fig. 6a) or deep grooves[95]. Such systems can even be scaled down to nanometre dimensions, as demonstrated by studies of thermal radiation from individual subwavelength (in width) infrared resonant antennas[96] and electrically driven platinum microheaters[97]. These types of plasmonic light-concentrating structure may form the basis of a new class of infrared light sources.

Alternative material systems may also prove useful for constructing infrared emitters. Doped semiconductors, which possess carrier concentrations that are orders of magnitude smaller than in metals, can exhibit surface plasmon resonances (when $\varepsilon = -1$) at infrared frequencies[98]. Silicon carbide (SiC) can support a different type of surface wave, a surface phonon polariton, at frequencies near the transverse optical phonon resonance. By etching gratings into a SiC surface, researchers have made thermal sources that exhibit narrow angular emission lobes[99] (Fig. 6c). The properties of structured thermal emitters are particularly striking in the near-field regime, where the LDOS can differ drastically from that in a vacuum. The thermal energy density near a SiC surface (Fig. 6b), for example, is strongly peaked at the surface phonon polariton resonance frequency ($\varepsilon = -1$), and decays away from the surface with a $1/z^3$ dependence[100], where z is the distance from the surface. Using thermal-radiation scanning tunnelling microscopy, researchers have tapped into this energy density and mapped out the thermal near-fields of various plasmonic structures[101] (Fig. 6d). The ability to probe thermal near-fields is particularly relevant to the study of heat transport at the nanoscale.

At thermal equilibrium the thermal near-fields discussed above are 'bound' to the structure in question and no energy is transported or radiated away. However, if a colder object is brought within the near-field, photons can tunnel between the two objects and create new radiation pathways. At small distances this form of radiative energy transfer can be larger in magnitude than the power radiated into the far-field, and potentially can even transport energy more efficiently than direct thermal conduction[102]. As an example, take the case of a spherical polarizable object located a short distance away from a planar surface. Analytical solutions for the power radiated in this geometry[103] reveal strong near-field contributions to the heat transfer owing to both localized surface resonances in the particle ($\varepsilon = -2$) and surface wave resonances of the substrate ($\varepsilon = -1$). Furthermore, the radiated power decays with the familiar $1/z^3$ dependence. This simple model can approximate the heat transfer between a scanning probe tip and an underlying sample. Recent experiments on the heat transfer between a heated scanning tunnelling microscopy tip and cooled sample at various tip–sample separations agree well with theoretical calculations for distances larger than 10 nm (Fig. 6e; ref. 104). Studies of near-field thermal radiation are redefining our understanding of nanoscale heat transport and may lead to new techniques for managing heat in emerging nanotechnologies.

Metamaterials

The ability of deep-subwavelength plasmonic structures to show strong light–matter interactions is forming the basis of an entirely new class of optical materials. When arranged into periodic arrays, metallic structures can act as the functional units of an artificial medium known as a metamaterial. When the scale of inhomogeneity in the medium is significantly smaller than the wavelength of light, the electromagnetic radiation fails to resolve the fine features of the plasmonic building blocks, and the electromagnetic response of the system can be described by bulk, macroscopic parameters such as ε and permeability (μ). By properly engineering the underlying subunits, metamaterials can exhibit exotic optical properties that are not attainable in naturally occurring materials, such as prominent magnetic response[105], negative index of refraction[106], the giant chiral effect[107], as well as many more.

By removing conventional constraints on realizable properties in optical materials, metamaterials have enabled the objective-oriented design of optical technologies using transformation optics. Originating from the form-invariance of Maxwell's equations under coordinate transformations[108], transformation optics allows

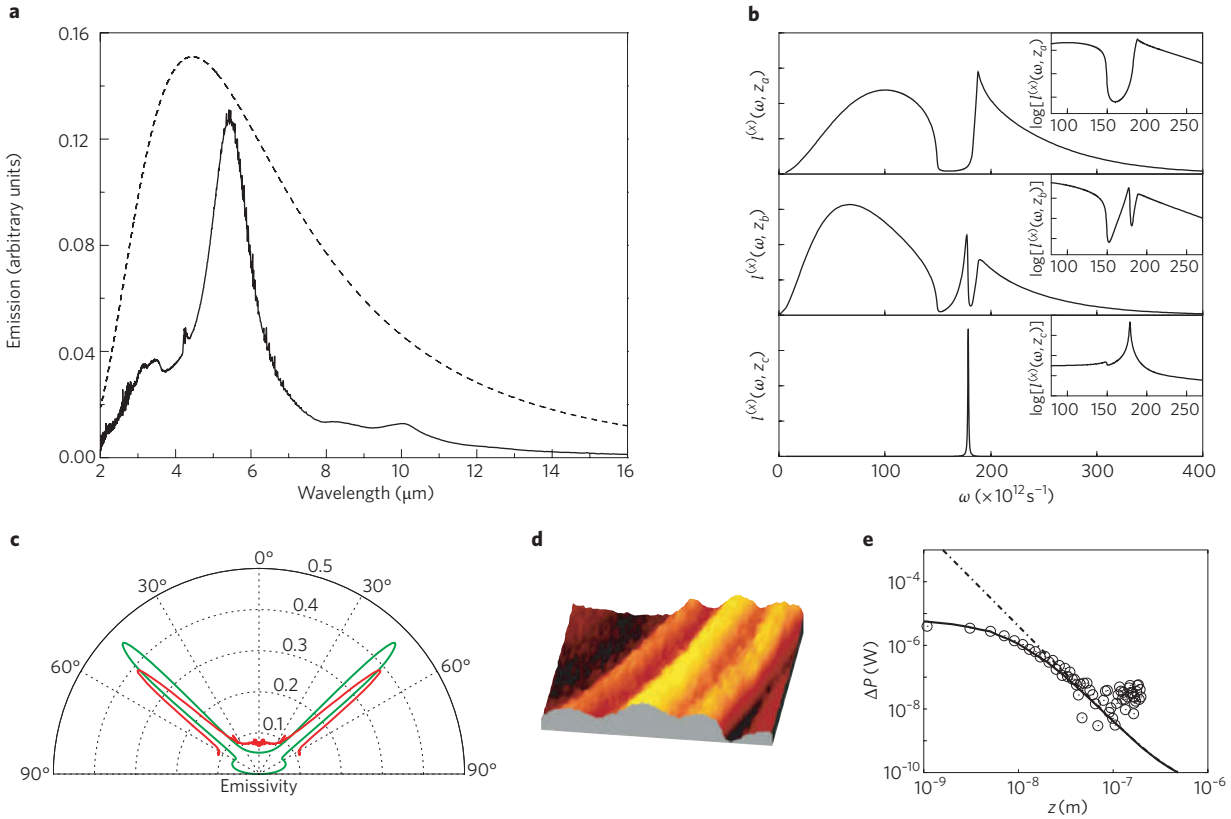

Figure 6 | Engineering thermal emitters. a, Thermal emission from an array of microstrip patches (solid line) compared with a black-body of the same temperature (dotted line) as a function of wavelength[93]. **b**, Thermal energy density (I, expressed in arbitrary units) above a SiC surface at a distance of z_a = 1,000 μm (top), z_b = 2 μm (middle), and z_c = 0.1 μm (bottom). At small distances there is a peak near 179 THz (10.5 μm) owing to the contribution of surface phonon polaritons[99]. Inset: the same data on a logarithmic vertical axis. **c**, Experimental (red) and theoretical (green) emissivity for 11.36-μm p-polarized light emanating from a SiC grating. The grating out-couples surface phonon polaritons into a narrow emission lobe[98]. **d**, Thermal-radiation scanning tunnelling microscopy image of 10.9-μm-wavelength near-field energy density above a gold stripe, revealing SPP interference fringes[100]. **e**, Experimental (circles) and theoretical (lines) heat flux (ΔP) between a metal tip and GaN surface. The dashed line shows the z^{-3} dependence described in the text. The solid line is a phenomenological model that describes departures from the ideal case at small distances[103]. Figures reproduced with permission: **a**, © 2008 AIP; **b**, © 2000 APS; **c**, © 2002 NPG; **d**, © 2006 NPG; **e**, © 2005 APS.

researchers to distort 'optical space' and mould the flow of light in an unprecedented fashion. Many of the unusual optical phenomena observed in recent years, including negative refraction or the actions of a perfect lens[109] or hyperlens[110], can be viewed as special cases of transformation optics. Several transformation-based devices, especially electromagnetic cloaks[111], have been theoretically proposed and experimentally demonstrated at both microwave and optical frequencies[112–114].

The first step of transformation optics is to envision a distortion of real space that results in a desired functionality. Second, the given spatial distortion is translated into a specific spatial transformation, which determines the required ε and μ tensors. Finally, and the most serious difficulty of all, realistic design and fabrication constraints for the required materials properties are incorporated to eventually realize the design. An example of the application of transformation optics towards the design of a macroscopic light concentrator[115] is given in Box 1. As the example shows, transformation optics is a powerful technique for translating an imagined optical effect into a realizable technology.

Outlook

The field of plasmonics has grown dramatically over the past decade and new directions are continuously emerging. This review has provided only a brief snapshot of some exciting areas in plasmonics. As shown by the material in the various subsections, the subset of plasmonic structures that use extreme light concentration and manipulation are witnessing particularly rapid developments and show significant future promise. We hope this review has provided a valuable perspective and will help inspire the next wave of plasmonic science and technologies.

References

1. Anker, J. N. *et al.* Biosensing with plasmonic nanosensors. *Nature Mater.* **7,** 442–453 (2008).
2. Wang, F. & Shen, Y. R. General properties of local plasmons in metal nanostructures. *Phys. Rev. Lett.* **97,** 206806 (2006).
3. Stockman, M. I., Shalaev, V. M., Moskovits, M., Botet, R. & George, T. F. Enhanced Raman scattering by fractal clusters: Scale-invariant theory. *Phys. Rev. B.* **46,** 2821–2830 (1992).
4. Li, K. R., Stockman, M. I. & Bergman, D. J. Self-similar chain of metal nanospheres as an efficient nanolens. *Phys. Rev. Lett.* **91,** 227402 (2003).
5. Novotny, L. Effective wavelength scaling for optical antennas. *Phys. Rev. Lett.* **98,** 266802 (2007).
6. Bryant, G., Garcia de Abajo, F. J. & Aizpurua, J. Mapping the plasmon resonances of metallic nanoantennas. *Nano Lett.* **8,** 631–636 (2008).
7. Ditlbacher, H. *et al.* Silver nanowires as surface plasmon resonators. *Phys. Rev. Lett.* **95,** 257403 (2005).
8. Søndergaard, T. & Bozhevolnyi, S. I. Slow-plasmon resonant nanostructures: Scattering and field enhancements. *Phys. Rev. B* **75,** 073402 (2007).
9. Søndergaard, T. & Bozhevolnyi, S. I. Metal nano-strip optical resonators. *Opt. Express* **15,** 4198–4204 (2007).
10. Barnard, E. S., White, J. S., Chandran, A. & Brongersma, M. L. Spectral properties of plasmonic resonator antennas. *Opt. Express* **16,** 16529–16537 (2008).
11. Miyazaki, H. T. & Kurokawa, Y. Squeezing visible light waves into a 3-nm-thick and 55-nm-long plasmon cavity. *Phys. Rev. Lett.* **96,** 097401 (2006).

12. Thio, T., Pellerin, K. M., Linke, R. A., Lezec, H. J. & Ebbesen, T. W. Enhanced light transmission through a single subwavelength aperture. *Opt. Lett.* **26,** 1972–1974 (2001).
13. Ditlbacher, H., Krenn, J. R., Hohenau, A., Leitner, A. & Aussenegg, F. R. Efficiency of local light-plasmon coupling. *Appl. Phys. Lett.* **83,** 3665–3667 (2003).
14. Schuck, P. J., Fromm, D. P., Sundaramurthy, A., Kino, G. S. & Moerner, W. E. Improving the mismatch between light and nanoscale objects with gold bowtie nanoantennas. *Phys. Rev. Lett.* **94,** 017402 (2005).
15. Gersten, J. & Nitzan, A. Electromagnetic theory of enhanced Raman scattering by molecules adsorbed on rough surfaces. *J. Chem. Phys.* **73,** 3023–3037 (1980).
16. Stockman, M. I. Nanofocusing of optical energy in tapered plasmonic waveguides. *Phys. Rev. Lett.* **93,** 137404 (2004).
17. Verhagen, E., Spasenovic, M., Polman, A. & Kuipers, L. Nanowire plasmon excitation by adiabatic mode transformation. *Phys. Rev. Lett.* **102,** 203904 (2009).
18. Bethe, H. A. Theory of diffraction by small holes. *Phys. Rev.* **66,** 163–182 (1944).
19. Shi, X. & Hesselink, L. Mechanisms for enhancing power throughput from planar nano-apertures for near-field optical data storage. *Jpn. J. Appl. Phys.* **41,** 1632–1635 (2002).
20. Novotny, L., Bian, R. X. & Xie, X. S. Theory of nanometric optical tweezers *Phys. Rev. Lett.* **79,** 645–648 (1997).
21. Challener, W. A. *et al.* Heat-assisted magnetic recording by a near-field transducer with efficient optical energy transfer. *Nature Photon.* **3,** 220–224 (2009).
22. Srituravanich, W. *et al.* Flying plasmonic lens in the near-field for high-speed nanolithography. *Nature Nanotech.* **3,** 733–737 (2008).
23. Huber, A. J. *et al.* Terahertz near-field nanoscopy of mobile carriers in single semiconductor nanodevices. *Nano Lett.* **8,** 3766–3770 (2008).
24. Hartschuh, A., Sanchez, E. J., Xie, X. S. & Novotny, L. High-resolution near-field Raman microscopy of single-walled carbon nanotubes. *Phys. Rev. Lett.* **90,** 095503 (2003).
25. Frey, H., Witt, S., Felderer, K. & Guckenberger, R. High-resolution imaging of single fluorescent molecules with the optical near-field of a metal tip. *Phys. Rev. Lett.* **93,** 200801 (2004).
26. Kalkbrenner, T., Ramstein, M., Mlynek, J. & Sandoghar, V. A single gold particle as a probe for apertureless scanning near-field optical microscopy. *J. Microsc.* **202,** 72–76 (2001).
27. Farahani, J. N., Pohl, D. W., Eisler, H. J. & Hecht, B. Single quantum dot coupled to a scanning optical antenna: A tunable superemitter. *Phys. Rev. Lett.* **95,** 017402 (2005).
28. Taminiau, T. H. *et al.* λ/4 resonance of an optical monopole antenna probed by single molecule fluorescence. *Nano Lett.* **7,** 28–33 (2007).
29. Barwicz, T. *et al.* Silicon photonics for compact, energy-efficient interconnects [Invited]. *J. Opt. Netw.* **6,** 63–73 (2007).
30. White, J. S. *et al.* Extra-ordinary optical absorption through sub-wavelength slits. *Opt. Lett.* **34,** 686–688 (2009).
31. Ishi, T., Fujikata, T., Makita, K., Baba, T. & Ohashi, K. Si nano-photodiode with a surface plasmon antenna. *Jpn. J. Appl. Phys.* **44,** 364–366 (2005).
32. Tang, L. *et al.* Nanometre-scale germanium photodetector enhanced by a near-infrared dipole antenna. *Nature Photon.* **2,** 226–229 (2008).
33. Ditlbacher, H. *et al.* Organic diodes as monolithically integrated surface plasmon polariton detectors. *Appl. Phys. Lett.* **89,** 161101 (2006).
34. Neutens, P., Van Dorpe, P., De Vlaminck, I., Lagae, L. & Borghs, G. Electrical detection of confined gap plasmons in metal-insulator-metal waveguides. *Nature Photon.* **3,** 283–286 (2009).
35. Ly-Gagnon, D. S., Kocabas, S. E. & Miller, D. A. B. Characteristic impedance model for plasmonic metal slot waveguides. *IEEE J. Quantum Electron.* **14,** 1473–1478 (2008).
36. Laux, E., Genet, C., Skauli, T. & Ebbesen, T. W. Plasmonic photon sorters for spectral and polarimetric imaging. *Nature Photon.* **2,** 161–164 (2008).
37. Nikolajsen, T., Leosson, K. & Bozhevolnyi, S. I. Surface plasmon polariton modulators and switches operating at telecom wavelengths. *Appl. Phys. Lett.* **85,** 5833–5835 (2004).
38. Cai, W., White, J. S. & Brongersma, M. L. High-speed and power-efficient electrooptic plasmonic modulators. *Nano Lett.* **9,** 4403–4411 (2009).
39. Krasavin, A. V. & Zheludev, N. I. Active plasmonics: Controlling signals in Au/Ga waveguide using nanoscalestructural transformations. *Appl. Phys. Lett.* **84,** 1416–1418 (2004).
40. Dintinger, J., Robel, I., Kamat, P. V., Genet, C. & Ebbesen, T. W. Terahertz all-optical molecule-plasmon modulation. *Adv. Mater.* **18,** 1645–1648 (2006).
41. Pacifici, D., Lezec, H. J. & Atwater, H. A. All-optical modulation by plasmonic excitation of CdSe quantum dots. *Nature Photon.* **1,** 402–406 (2007).
42. Pala, R. A., Shimizu, K. T., Melosh, N. A. & Brongersma, M. L. A nonvolatile plasmonic switch employing photochromic molecules. *Nano Lett.* **8,** 1506–1510 (2008).
43. Dicken, M. J. *et al.* Electrooptic modulation in thin film barium titanate plasmonic interferometers. *Nano Lett.* **8,** 4048–4052 (2008).
44. MacDonald, K. F., Sámson, Z. L., Stockman, M. I. & Zheludev, N. I. Ultrafast active plasmonics. *Nature Photon.* **3,** 55–58 (2009).
45. Shen, Y. & Wang, G. P. Optical bistability in metal gap waveguide nanocavities. *Opt. Express* **16,** 8421–8426 (2008).
46. Green, M. A. Recent developments in photovoltaics. *Sol Energy* **76,** 3–8 (2004).
47. Atwater, H. A. & Polman, A. Plasmonics for improved photovoltaic devices. *Nature Mater.* **9,** 205–213 (2010).
48. Kume, T. *et al.* Enhancement of photoelectric conversion efficiency in copper phthalocyanine solar cell: white light excitation of surface plasmon polaritons. *Jpn. J. Appl. Phys.* **34,** 6448–6451 (1995).
49. Stenzel, O. *et al.* Enhancement of the photovoltaic conversion efficiency of copper phthalocyanine thin film devices by incorporation of metal clusters. *Sol. Energy Mater. Sol. Cells* **37,** 337–348 (1995).
50. Pala, R. A., White, J., Barnard, E., Liu, J. & Brongersma, M. L. Design of plasmonic thin-film solar cells with broadband absorption enhancements. *Adv. Mater.* **21,** 3504–3509 (2009).
51. Catchpole, K. R. & Polman, A. Design principles for particle plasmon enhanced solar cells. *Appl. Phys. Lett.* **93,** 191113 (2008).
52. Nitzan, A. & Brus, L. E. Theoretical model for enhanced photochemistry on rough surfaces. *J. Chem. Phys.* **75,** 2205–2214 (1981).
53. Chen, C. J. & Osgood, R. M. Direct observation of the local-field-enhanced surface photochemical reactions *Phys. Rev. Lett.* **50,** 1705–1708 (1983).
54. Shimizu, K. T., Pala, R. A., Fabbri, J. D., Brongersma, M. L. & Melosh, N. A. Probing molecular junctions using surface plasmon resonance spectroscopy. *Nano Lett.* **6,** 2797–2803 (2006).
55. Novo, C., Funston, A. M. & Mulvaney, P. Direct observation of chemical reactions on single gold nanocrystals using surface plasmon spectroscopy. *Nature Nanotech.* **3,** 598–602 (2008).
56. Baffou, G., Quidant, R. & Girard, C. Heat generation in plasmonic nanostructures: influence of morphology. *Appl. Phys. Lett.* **94,** 153109 (2009).
57. Baffou, G., Kreuzer, M. P., Kulzer, F. & Quidant, R. Temperature mapping near plasmonic nanostructures using fluorescence polarization anisotropy. *Opt. Express* **17,** 3291–3298 (2009).
58. Hirsch, L. R. *et al.* Nanoshell-mediated near-infrared thermal therapy of tumours under magnetic resonance guidance. *Proc. Natl Acad. Sci. USA* **100,** 13549–13554 (2003).
59. Rontzsch, L., Heinig, K. H., Schuller, J. A. & Brongersma, M. L. Thin film patterning by surface-plasmon-induced thermocapillarity. *Appl. Phys. Lett.* **90,** 044105 (2007).
60. Govorov, A. O. *et al.* Gold nanoparticles ensembles as heaters and actuators: melting and collective plasmon resonances. *Nanoscale Res. Lett.* **1,** 84–90 (2006).
61. Soares, B. F., Jonsson, F. & Zheludev, N. I. All-optical phase-change memory in a single gallium nanoparticle. *Phys. Rev. Lett.* **98,** 153905 (2007).
62. Cao, L., Barsic, D. N., Guichard, A. R. & Brongersma, M. L. Plasmon-assisted local temperature control to pattern individual semiconductor nanowires and carbon nanotubes. *Nano Lett.* **7,** 3523–3527 (2007).
63. Boyd, D. A., Adleman, J. R., Goodwin, D. G. & Psaltis, D. Chemical separations by bubble-assisted interphase mass-transfer. *Anal. Chem.* **80,** 2452–2456 (2008).
64. Sershen, S. R., Wescott, S. L., Halas, N. J. & West, J. L. Temperature-sensitive polymer-nanoshell composites for photothermally modulated drug delivery. *J. Biomed. Mater. Res. A* **51,** 293–298 (2000).
65. Reismann, M., Bretschneider, J. C., von Plessen, G. & Simon, U. Reversible photothermal melting of DNA in DNA-gold-nanoparticle networks. *Small* **4,** 607–610 (2008).
66. Stehr, J. *et al.* Gold nanostoves for microsecond DNA melting analysis. *Nano Lett.* **8,** 619–623 (2008).
67. Simon, H. J., Mitchell, D. E. & Watson, J. G. Optical second-harmonic generation with surface plasmons in silver films. *Phys. Rev. Lett.* **33,** 1531–1534 (1974).
68. Nahata, A., Linke, R. A., Ishi, T. & Ohashi, K. Enhanced nonlinear optical conversion from a periodically nanostructured metal film. *Opt. Lett.* **28,** 423–425 (2003).
69. Lesuffleur, A., Kumar, L. & Gordon, R. Enhanced second harmonic generation from nanoscale double-hole arrays in a gold film. *Appl. Phys. Lett.* **88,** 261104 (2006).
70. Van Nieuwstadt, J. A. H. *et al.* Strong modification of the nonlinear optical response of metallic subwavelength hole arrays. *Phys. Rev. Lett.* **97,** 146102 (2006).
71. Xu, T., Jiao, X., Zhang, G.-P. & Blair, S. Second-harmonic emission from subwavelength apertures: Effects of aperture symmetry and lattice arrangement. *Opt. Express* **15,** 13894–13906 (2007).
72. Fan, W. *et al.* Second harmonic generation from a nanopatterned isotropic nonlinear material. *Nano Lett.* **6,** 1027–1030 (2006).
73. Fan, W. *et al.* Second harmonic generation from patterned GaAs inside a subwavelength metallic hole array. *Opt. Express* **14,** 9570–9575 (2006).

74. Kim, S. *et al.* High-harmonic generation by resonant plasmon field enhancement. *Nature* **453,** 757–760 (2008).
75. Anger, P., Bharadwaj, P. & Novotny, L. Enhancement and quenching of single-molecule fluorescence. *Phys. Rev. Lett.* **96,** 113002 (2006).
76. Kuhn, S., Hakanson, U., Rogobete, L. & Sandoghdar, V. Enhancement of single-molecule fluorescence using a gold nanoparticle as an optical nanoantenna. *Phys. Rev. Lett.* **97,** 017402 (2006).
77. Muskens, O. L. *et al.* Strong enhancement of the radiative decay rate of emitters by single plasmonic nanoantennas. *Nano Lett.* **7,** 2871–2875 (2007).
78. Mertens, H., Koenderink, A. F. & Polman, A. Plasmon-enhanced luminsecence near noble-metal nanospheres: comparison of exact theory and an improved Gersten and Nitzan model. *Phys. Rev. B* **76,** 115123 (2007).
79. Taminiau, T. H., Stefani, F. D., Segerink, F. B. & Van Hulst, N. F. Optical antennas direct single-molecule emission. *Nature Photon.* **2,** 234–237 (2008).
80. Wenger, J. *et al.* Emission and excitation contributions to enhance single molecule fluorescence by gold nanometric apertures. *Opt. Express* **16,** 3008–3020 (2008).
81. Levene, M. J. *et al.* Zero-mode waveguides for single-molecule analysis at high concentrations. *Science* **299,** 682–686 (2003).
82. Neogi, A. *et al.* Enhancement of spontaneous recombination rate in a quantum well by resonant surface plasmon coupling. *Phys. Rev. B* **66,** 153305 (2002).
83. Okamoto, K. *et al.* Surface-plasmon-enhanced light emitters based on InGaN quantum wells. *Nature Mater.* **3,** 601–605 (2004).
84. Jun, Y. C., Kekatpure, R. D., White, J. S. & Brongersma, M. L. Nonresonant enhancement of spontaneous emission in metal-dielectric-metal plasmon waveguide structures. *Phys. Rev. B* **78,** 153111 (2008).
85. Chang, D. E., Sorensen, A. S., Haemmer, P. R. & Lukin, M. D. Quantum optics with surface plasmons. *Phys. Rev. Lett.* **97,** 053002 (2006).
86. Chang, D. E., Sorensen, A. S., Demler, E. A. & Lukin, M. D. A single-photon transistor using nanoscale surface plasmons. *Nature Phys.* **3,** 807–812 (2007).
87. Akimov, A. V. *et al.* Generation of single optical plasmons in metallic nanowires coupled to quantum dots. *Nature* **450,** 402–406 (2007).
88. Hill, M. T. *et al.* Lasing in metallic-coated nanocavities. *Nature Photon.* **1,** 589–594 (2007).
89. Hill, M. T. *et al.* Lasing in metal-insulator-metal sub-wavelength plasmonic waveguides. *Opt. Express* **17,** 11107–11112 (2009).
90. Oulton, R. F. *et al.* Plasmon lasers at deep subwavelength scale. *Nature* **461,** 629–632 (2010).
91. Bergman, D. J. & Stockman, M. I. Surface plasmon amplification by stimulated emission of radiation: quantum generation of coherent surface plasmons in nanosystems. *Phys. Rev. Lett.* **90,** 027402 (2003).
92. Stockman, M. I. Spasers explained. *Nature Photon.* **2,** 327–329 (2008).
93. Noginov, M. A. Demonstration of a spaser-based nanolaser. *Nature* **460,** 1110–1112 (2009).
94. Puscasu, I. & Schaich, W. L. Narrow-band, tunable infrared emission from arrays of microstrip patches. *Appl. Phys. Lett.* **92,** 233102 (2008).
95. Miyazaki, H. T. *et al.* Thermal emission of two-colour polarized infrared waves from integrated plasmon cavities. *Appl. Phys. Lett.* **92,** 141114 (2008).
96. Schuller, J. A., Taubner, T. & Brongersma, M. L. Optical antenna thermal emitters. *Nature Photon.* **3,** 658–661 (2009).
97. Au, Y. Y. Thermal radiation spectra of individual subwavelength microheaters. *Phys. Rev. B* **78,** 085402 (2008).
98. Marquier, F. *et al.* Engineering infrared emission properties of silicon in the near and far field. *Opt. Commun.* **237,** 379–388 (2004).
99. Greffet, J. J. *et al.* Coherent emission of light by thermal sources. *Nature* **416,** 61–64 (2002).
100. Shchegrov, A. V., Joulain, K., Carminati, R. & Greffet, J. J. Near-field spectral effects due to electromagnetic surface excitations. *Phys. Rev. Lett.* **85,** 1548–1551 (2000).
101. Wilde, Y. D. *et al.* Thermal radiation scanning tunneling microscopy. *Nature* **444,** 740–743 (2006).
102. Volokitin, A. I. & Persson, B. N. J. Near-field radiative heat transfer and non-contact friction. *Rev. Mod. Phys.* **79,** 1291–1329 (2007).
103. Mulet, J. P., Joulain, K., Carminati, R. & Greffet, J. J. Nanoscale radiative heat transfer between a small particle and a plane surface. *Appl. Phys. Lett.* **78,** 2931–2933 (2001).
104. Kittel, A. *et al.* Near-field heat transfer in a scanning thermal microscope. *Phys. Rev. Lett.* **95,** 224301 (2005).
105. Cai, W. S. *et al.* Metamagnetics with rainbow colours. *Opt. Express* **15,** 3333–3341 (2007).
106. Shalaev, V. M. Optical negative-index metamaterials. *Nature Photon.* **1,** 41–48 (2007).
107. Plum, E. *et al.* Giant optical gyrotropy due to electromagnetic coupling. *Appl. Phys. Lett.* **90,** 223113 (2007).
108. Ward, A. J. & Pendry, J. B. Refraction and geometry in Maxwell's equations. *J. Mod. Opt.* **43,** 773–793 (1996).
109. Pendry, J. B. Negative refraction makes a perfect lens. *Phys. Rev. Lett.* **85,** 3966–3969 (2000).
110. Jacob, Z., Alekseyev, L. V. & Narimanov, E. Optical hyperlens: Far-field imaging beyond the diffraction limit. *Opt. Express* **14,** 8247–8256 (2006).
111. Pendry, J. B., Schurig, D. & Smith, D. R. Controlling electromagnetic fields. *Science* **312,** 1780–1782 (2006).
112. Schurig, D. *et al.* Metamaterial electromagnetic cloak at microwave frequencies. *Science* **314,** 977–980 (2006).
113. Cai, W. S., Chettiar, U. K., Kildishev, A. V. & Shalaev, V. M. Optical cloaking with metamaterials. *Nature Photon.* **1,** 224–227 (2007).
114. Valentine, J., Li, J., Zentgraf, T., Bartal, G. & Zhang, X. An optical cloak made of dielectrics. *Nature Mater.* **8,** 568–571 (2009).
115. Rahm, M. *et al.* Design of electromagnetic cloaks and concentrators using form-invariant coordinate transformations of Maxwell's equations. *Photonic. Nanostruct.* **6,** 87–95 (2008).
116. Bohren, C. F. & Huffman, D. R. *Absorption and Scattering of Light by Small Particles* (Wiley Inter-Science, 1998).
117. Verhagen, E., Polman, A. & Kuipers, L. K. Nanofocusing in laterally tapered plasmonic waveguides. *Opt. Express* **16,** 45–57 (2008).
118. Mühlschlegel, P., Eisler, H. J., Martin, O. J. F., Hecht, B. & Pohl, D. W. Resonant optical antennas. *Science* **308,** 1607–1609 (2005).
119. Schurig, D., Pendry, J. B. & Smith, D. R. Calculation of material properties and ray tracing in transformation media. *Opt. Express.* **14,** 9794–9804 (2006).
120. Cai, W. S. *et al.* Nonmagnetic cloak with minimized scattering. *Appl. Phys. Lett.* **91,** 111105 (2007).

Acknowledgements

The authors of this article would like to acknowledge support from a US Department of Defense Multidisciplinary University Research Initiative sponsored by the Air Force Office of Scientific Research (F49550-04-1-0437). The authors also thank the Centre on Nanostructuring for Efficient Energy Conversion, an Energy Frontier Research Center funded by the US Department of Energy, Office of Science, Office of Basic Energy Sciences under award number DE-SC0001060.

Additional information

The authors declare no competing financial interests.